

## Electronic supplementary information to

# Binding affinity data of DNA aptamers for therapeutic anthracyclines from microscale thermophoresis and surface plasmon resonance spectroscopy

Stephan Sass,<sup>a</sup> Walter F.M. Stöcklein,<sup>b</sup> Anja Klevesath,<sup>b</sup> Jeanne Hurpin,<sup>a</sup> Marcus Menger\*<sup>‡b</sup> and Carsten Hille\*<sup>‡a,c</sup>

<sup>a</sup>Physical Chemistry / ALS ComBi, Institute of Chemistry, University of Potsdam, 14476 Potsdam, Germany.

<sup>b</sup>Fraunhofer Institute for Cell Therapy and Immunology, Branch Bioanalysis and Bioprocesses (IZI-BB), 14476 Potsdam, Germany.

E-mail: marcus.menger@izi-bb.fraunhofer.de; Tel: +49 331 58187 316

<sup>c</sup>Technical University of Applied Sciences Wildau, 15745 Wildau, Germany.

E-mail: carsten.hille@th-wildau.de; Tel.: +49 3375 508 793

\* Corresponding authors.

‡ These authors contributed equally.

## Part 1 – Microscale thermophoresis

### Additional Results and Discussion

MST allows for quantitative analysis of the interaction between the anthracyclines and the oligonucleotides in free solution. For this, the concentration of the Cy5-labeled oligonucleotides, such as aptamer DRN-10, was kept constant, whereas the anthracycline concentration was varied. In order to study the specificity of the aptamers, a set of four chemotherapeutic and antibiotic substances was tested (Figure S1).

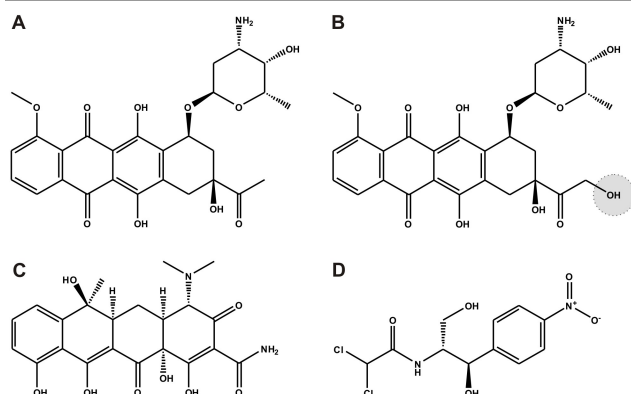


**Figure S1** Structures of the chemotherapeutic anthracyclines (A) daunorubicin and (B) doxorubicin shown with their slight structural difference as well as of the antibiotics (C) tetracycline and (D) chloramphenicol.

Typical thermophoresis curves are shown in Figure S2A. After 5 s of constant fluorescence intensity, indicating negligible photobleaching at the given LED power, a biphasic decrease in the fluorescence intensity was observed when generating the temperature gradient with the IR-laser. An initial fast decrease within ~1 s, the so called temperature jump (*T*-jump), is the result of the intrinsic temperature-dependent change in the fluorescence.<sup>1,2</sup> The diffusion-limited motion of molecules within the temperature gradient, the so-called thermophoresis, resulted in a subsequent slower decrease within several seconds. After disrupting the temperature gradient, an inverted *T*-jump as well as back-diffusion of molecules can be observed. An increase in the daunorubicin concentration up to 100 nM resulted in an enhanced

decrease in the fluorescence intensity when maintaining the temperature gradient (positive thermophoresis), as indicated by green colour code (Figure S2A, *inset*). This concentration regime indicates the aptamer-specific binding to daunorubicin. However, further increase in daunorubicin concentration up to 1  $\mu$ M resulted in an opposing behaviour (negative thermophoresis), as indicated by blue colour code (Figure S2A, *inset*). Indeed, daunorubicin is known for nonspecific intercalation into DNA with low affinity of approx.  $2 \times 10^{-4}$  M for single-stranded DNA, inducing this opposing behaviour.<sup>3</sup>

For binding analysis, the fluorescence intensities were calculated for the period before and during the established temperature gradient and from this the normalised fluorescence  $\Delta F_{\text{norm}}$  was calculated. However, binding curves can be obtained by analysing the *T*-jump, the thermophoresis or both effects by choosing the respective time windows from the MST thermophoresis curves (Figure S2B). All three analysis algorithms resulted in the same trend of the binding curve, unravelling the decrease in  $\Delta F_{\text{norm}}$  up to 100 nM daunorubicin and a subsequent increase in  $\Delta F_{\text{norm}}$  at higher daunorubicin concentrations. Obviously, the unspecific intercalation of more than one daunorubicin molecules into the DNA leads to dramatic changes in the size, charge or hydration shell in comparison to the specific binding of one daunorubicin molecule to the DNA aptamer. Analysis of the specific binding resulted in  $K_D$ -values of  $3.2 \text{ nM} \pm 1.0 \text{ nM}$ ,  $4.8 \text{ nM} \pm 2.6 \text{ nM}$  and  $4.3 \text{ nM} \pm 1.5 \text{ nM}$  (each  $N = 3$ ) for using *T*-jump, thermophoresis and both effects, respectively. So, no significant differences could be observed in the  $K_D$ -values. However, the analysis of both effects resulted in the largest changes in  $\Delta F_{\text{norm}}$  leading to more reliable data analysis. Thus, in the performed MST recordings both effects were taken into account for  $K_D$  determination.

An 80 nt control DNA oligonucleotide (Con1) showed sequence similarities with the full-length aptamer DRN-10, but in the core sequence, several bases were substituted. Con1 exhibits G-quadruplex structures (see Figure 4), thought as prerequisite for binding, but neither daunorubicin nor doxorubicin showed specific binding to Con1. Only the unspecific intercalation at higher concentrations could be observed (Figure S3).

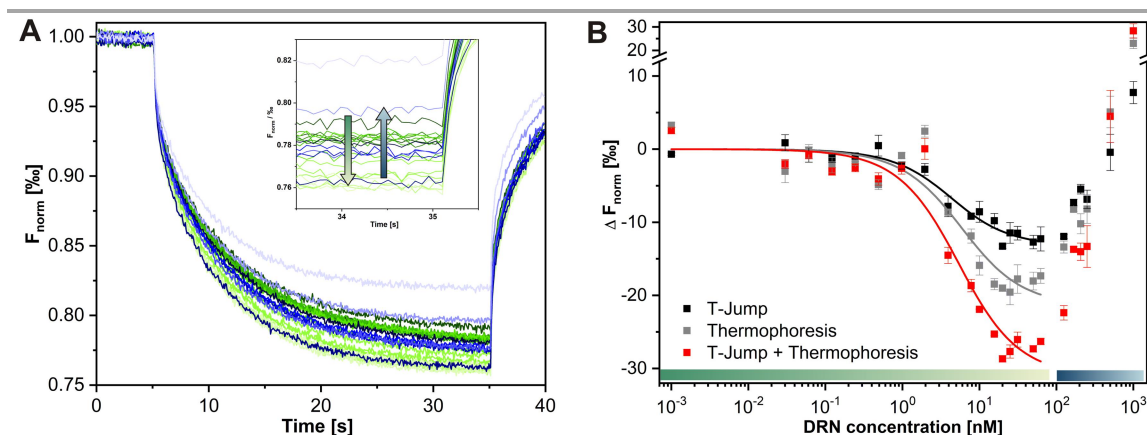


**Figure S2** Microscale thermophoresis (MST) data. **(A)** Normalised time traces from a representative MST experiment of 2 nM Cy5-labelled daurorubicin aptamer DRN-10 with 23 varying daurorubicin (DRN) concentrations (0-1.5  $\mu$ M). The green colour code indicates the decrease of  $\Delta F_{\text{norm}}$  up to 100 nM DRN and the blue colour code indicates the increase in  $\Delta F_{\text{norm}}$  at >100 nM DRN (*inset*). **(B)** Binding curves for aptamer DRN-10 and ligand DRN analysed from T-jump, thermophoresis or both effects; means  $\pm$  SEM,  $N = 3$ . The lines show the fit of data to the 1:1 binding model. The colour columns indicate the specific and unspecific DRN-binding as indicated in A.

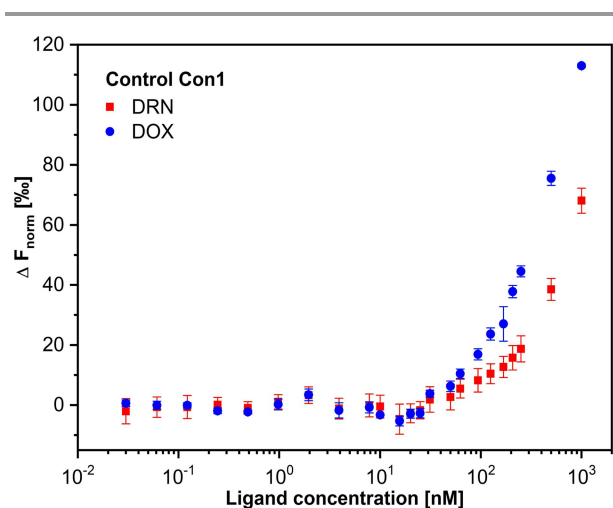


**Figure S3** MST binding analysis of the control DNA oligonucleotide Con1. Binding curves for Con1 and the two anthracyclines daurorubicin (DRN) and doxorubicin (DOX) analysed from T-jump and thermophoresis; means  $\pm$  SEM,  $N = 3$ .

## Part 2 – Fluorescence correlation spectroscopy

### Experimental

Fluorescence correlation spectroscopy (FCS) measurements were performed using a MicroTime 200 time-resolved confocal fluorescence microscope (PicoQuant, Berlin, Germany) with excitation at  $\lambda_{\text{ex}} = 470$  nm (LDH-P-C-470, repetition rate 20 MHz, pulse width <90 ps). Excitation light was focused into the solution via an Olympus PlanApo 100 $\times$ /NA1.4 oil immersion objective. Emission light was separated by a dichroic mirror, guided through a 50- $\mu$ m pinhole and a long pass filter LP 500 and was detected by two single-photon avalanche diodes (Perkin Elmer, USA). Samples of 50  $\mu$ l were measured in aptamer buffer for 30 min at 22  $^{\circ}$ C. Daurorubicin was kept constant at 10 nM and DRN-10 was titrated from 0 nM – 2,000 nM. Data were collected using the TCSPC electronics PicoHarp 300 and analysed using the software SymPhoTime 64 (PicoQuant).

The autocorrelation curves  $G(\tau)$  were calculated by crosscorrelating photons from the two different single-photon avalanche photodiodes. The focal volume was determined with 1 nM rhodamine 6G in water with known diffusion coefficient<sup>4</sup> yielding  $\kappa = 8.4 \pm 2.1$  ( $N = 3$ ). The normalised autocorrelation functions  $G(\tau)$  were fitted according to the standard model for 3-dimensional diffusion using Equation (S1):

$$G(\tau) = \frac{1}{N} \times \left(1 + \frac{\tau}{\tau_{\text{diff}}}\right)^{-1} \times \left(1 + \frac{\tau}{\kappa^2 \times \tau_{\text{diff}}}\right)^{-1/2} \quad (\text{S1})$$

where  $N$  is the average number of fluorescent molecules in the focal volume,  $\tau_{\text{diff}}$  is the diffusion time and  $\kappa$  is the structure parameter defining the shape of focal volume.<sup>5</sup>

### Results and Discussion

In addition to MST recordings, also FCS allows binding studies in free solution. Here, the fluorescence intensity fluctuations of labelled molecules are recorded during their diffusion through a small detection volume, normally <1 fl. However, only a substantial increase in the particle mass ( $m$ ) will result in a measurable effect on the diffusion time ( $\tau_{\text{diff}}$ ) due to  $\tau_{\text{diff}} \approx m^{1/3}$  according to Stokes-Einstein relation. Thus, the diffusion times of the interacting partners should differ by at least a factor of 1.6 under optimal conditions.<sup>6,7</sup>

According to these considerations, when analysing the interaction of an aptamer to a small molecule, the small molecule should be fluorescently labelled. However, labelling of small molecules such as daurorubicin can significantly change the binding properties to the aptamer. Fortunately, daurorubicin exhibits a broad fluorescence emission with a maximum at 590 nm when excited in the blue spectral range,<sup>8</sup> however, with quite low quantum yield leading to low signal count rates and long FCS recording times. The diffusion time of free daurorubicin in aptamer buffer was determined to  $\tau_{\text{diff}} = 32 \pm 7$   $\mu$ s and upon binding to DRN-10 the diffusion time increased by the factor of 3.3 to  $\tau_{\text{diff}} = 107 \pm 27$   $\mu$ s (Figure S4A). The increase in  $\tau_{\text{diff}}$  by factor of 3.3 fits to the mass difference of a factor

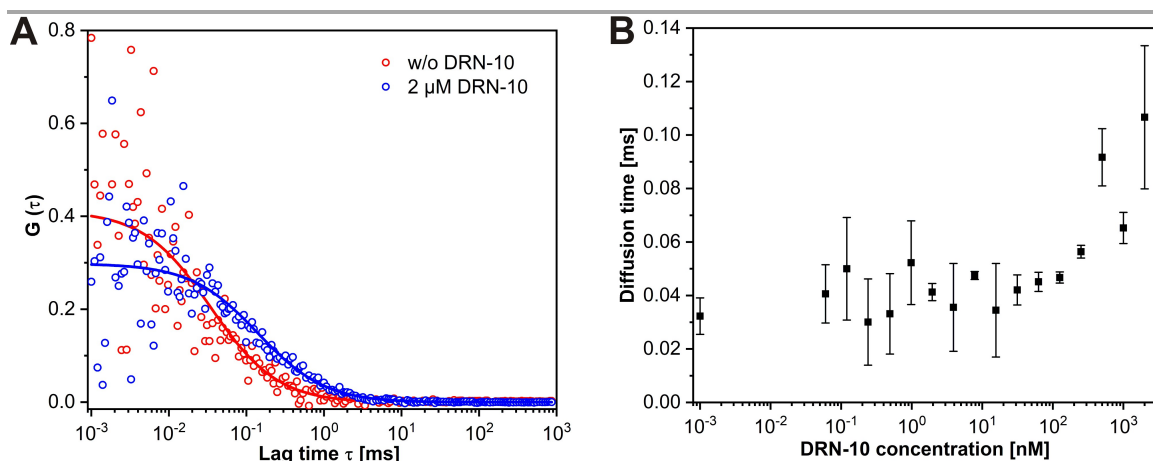


**Figure S4** Determination of binding properties of aptamer DRN-10 to daunorubicin by FCS. **(A)** Experimental (symbols) and fitted autocorrelation curves (lines) of daunorubicin in the absence (red) and presence (blue) of aptamer DRN-10. **(B)** Diffusion times of daunorubicin after the addition of different concentrations of aptamer DRN-10 derived from fits to a one-component 3D diffusion model; means  $\pm$  SEM. Data were derived from two independent experiments.

of 44 ( $M_{\text{daunorubicin}} = 564 \text{ g/mol}$  vs.  $M_{\text{DRN-10}} = 25.064 \text{ g/mol}$ ) due to  $\tau_{\text{diff}} \approx m^{1/3}$ . The change in  $\tau_{\text{diff}}$  was comparable to that of previously reported aptamer/molecule interactions.<sup>9,10</sup> Then, the diffusion times calculated from one-time-component analyses for different daunorubicin/DRN-10 ratios were thought to indicate binding, since the calculated diffusion time is the weighted average of the diffusion times of all diffusing daunorubicin molecules in solution. However, as shown in Figure S4B up to  $\sim 125 \text{ nM}$  DRN-10 no significant change in  $\tau_{\text{diff}}$  of daunorubicin could be observed, whereas an increase could be only seen at higher DRN-10 concentrations. According to the MST recordings (see Figure 1), only the unspecific intercalation of daunorubicin into the DNA could be resolved with FCS. The low fluorescence signal of daunorubicin seems to require a larger daunorubicin/aptamer mass difference of a factor of  $>500$  to resolve specific binding effects as postulated previously.<sup>6</sup> Thus, FCS recordings could be improved by coupling daunorubicin to a highly fluorescent label or by increasing the DRN-10 size significantly e.g. by coupling to PEG or dextrans.

## References

- 1 B. Zelent, T. Troxler and J. M. Vanderkooi, *J. Fluoresc.*, 2006, **17**, 37–42.
- 2 M. Jerabek-Willemsen, C. J. Wienken, D. Braun, P. Baaske and S. Duhr, *Assay Drug Dev. Technol.*, 2011, **9**, 342–353.
- 3 C. Gui-Fang, Z. Jie, T. Yong-Hua, H. Pin-Gang and F. Yu-Zhi, *Chinese J. Chem.*, 2005, **23**, 576–580.
- 4 C. B. Müller, A. Loman, V. Pacheco, F. Koberling, D. Willbold, W. Richtering and J. Enderlein, *EPL*, 2008, **83**, 46001.
- 5 A. J. García-Sáez and P. Schwille, *Methods*, 2008, **46**, 116–22.
- 6 U. Meseth, T. Wohland, R. Rigler and H. Vogel, *Biophys. J.*, 1999, **76**, 1619–31.
- 7 K. Bacia, S. A. Kim and P. Schwille, *Nat. Methods*, 2006, **3**, 83–89.
- 8 M. Than Htun, *J. Lumin.*, 2009, **129**, 344–348.
- 9 A. Werner, P. V. Konarev, D. I. Svergun and U. Hahn, *Anal. Biochem.*, 2009, **389**, 52–62.
- 10 H. Schürer, A. Buchynskyy, K. Korn, M. Famulok, P. Welzel and U. Hahn, *Biol. Chem.*, 2001, **382**, 479–81.